J Mater Sci (2009) 44:1407–1411
DOI 10.1007/s10853-009-3263-8

LETTER

Direct synthesis of carbon nanosheets by the solid-state pyrolysis of betaine

Athanasios B. Bourlinos · Theodore A. Steriotis · Radek Zboril · Vasilios Georgakilas · Athanasios Stubos

Received: 27 November 2008 / Accepted: 9 January 2009 / Published online: 30 January 2009

Carbon sheets of a few nanometers thick (nanosheets) define a peculiar class of carbon materials with unique surface-to-volume ratio, smooth surface morphologies and thin edges, flexibility and elasticity, high thermal and chemical stability, and lightness [1, 2]. In this respect, carbon nanosheets are promising candidates for hydrogen storage materials, sensors, catalyst supports, fillers, templates, and substrates for further functionalization and single graphene production [3–16]. In early studies, the particular carbon nanomaterials have been synthesized via radio-frequency or microwave plasma-enhanced chemical vapor deposition (CVD), expansion of graphite, chemical reduction of exfoliated graphite oxide, a solvothermal route, or catalytic growth [1–16]. However, these preparative methods suffer (depending on the case) from the following drawbacks: (i) low yield or/and concurrent formation of other carbon morphologies, which limits extensive studies and development; (ii) the thickness of the sheets rarely falls below 10 nm; (iii) from a technical standpoint, they often require a sophisticated apparatus, controlled atmosphere, high temperature, flammable gaseous mixtures, gas flow adjustments, time-consuming steps, catalysts, or highly corrosive and potentially explosive chemicals; and (iv) poor surface functionality, which restricts further derivatization. Unambiguously, the direct formation of customized carbon nanosheets at fairly good yields using simple and safe methods would be highly recommended from the viewpoint of commercial usage and applications.

Betaine, $(CH_3)_3N^+CH_2COO^-$, is an important zwitterionic organic compound widely distributed in nature. Although the thermal decomposition of betaine has been studied in detail [17, 18], nonetheless, there is no information available on the structure and morphology of the residual carbon after pyrolysis. To that end, herein we report the pyrolytic formation of ultrathin carbon nanosheets in air using betaine as a molecular precursor. This alternative yet paradox approach towards sheet-like carbons exhibits the following advantages: (i) it produces powder carbon nanosheets at fairly good yields; (ii) the thickness of the sheets is far less than 10 nm; (iii) the method is simple, safe, and inexpensive proceeding under normal conditions; and (iv) it directly introduces oxygen-containing functional groups in the solid, thus providing active sites to the surface for further modification. Overall, the present method offers new possibilities for the cost-efficient production and processing of this kind of materials.

Typically, 1 g of anhydrous betaine (Sigma) was calcined in air at 400 °C for 2 h at a heating rate of 10 °C min^{-1} to afford a lightweight, black-brown powder at 2% yield [17, 18] (Fig. 1). This sample, thereafter denoted as BET400, contains exclusively carbon nanosheets. The reported yield is sufficient enough for the preparation of bulk quantities of powder nanosheets (Fig. 1). Also note that calcination takes

A. B. Bourlinos (✉) · V. Georgakilas
Institute of Materials Science, NCSR "Demokritos", Ag. Paraskevi Attikis, Athens 15310, Greece
e-mail: bourlinos@ims.demokritos.gr

T. A. Steriotis
Institute of Physical Chemistry, NCSR "Demokritos", Ag. Paraskevi Attikis, Athens 15310, Greece

R. Zboril
Department of Physical Chemistry, Palacky University, Svobody 26, Olomouc 77146, Czech Republic

A. Stubos
Institute of Nuclear Technology and Radiation Protection, Environmental Research Laboratory, NCSR "Demokritos", Ag. Paraskevi Attikis, Athens 15310, Greece

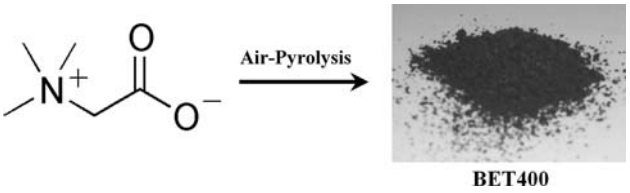

Fig. 1 Solid-state pyrolysis of betaine in air results in bulk quantities of powder carbon nanosheets

place well above the decomposition temperature of betaine (ca. 250 °C) [18]. Besides the present case study, the solid-state pyrolysis of other betaine compounds as above (e.g., betaine hydrochloride) also produced carbon nanosheets of similar dimensions, however, with much lower outputs (<0.5%). Elemental analysis (%): C, 60.84; H, 2.03; N, 5.26; O, 31.87, agrees with an average formula $C_{2.5}OHN_{0.19}$, which is close to that of graphite oxide [19, 20]. In view of their thickness and morphology, the as prepared nanosheets have a specific surface area of approximately 100 $m^2\ g^{-1}$ [5], measured by N_2 adsorption at 77 K (calculated by the Brunauer–Emmett–Teller method). The adsorption isotherm exhibits an H3 hysteresis loop, typical for plate-like particles [21]. Assuming that the surface area of individual graphene sheets is $\sim$2600 $m^2\ g^{-1}$ [5, 22], the measured value for BET400 corresponds to about 1/26 of the potential surface area. This means that the average thickness of the nanosheets should be about 9 nm ($\approx 26 \times 0.334$ nm). However, as we discuss below, this value actually corresponds to bundles of overlapped carbon nanosheets and not to individual specimens. Lastly, BET400 decomposes above 400 °C (based on TGA measurements under air), implying a relatively high thermal stability.

The XRD pattern of BET400 gives a broad (002) reflection centered at 3.6 Å, which agrees well with the formation of turbostratic carbon (Fig. 2, left). According to the Scherrer equation applied to the (002) reflection, the *c*-axis crystallite size was estimated at $L_c \sim 2$–3 nm. This suggests that individual nanosheets are indeed ultrathin, namely composed of stacks of 5–10 single layers in average. The

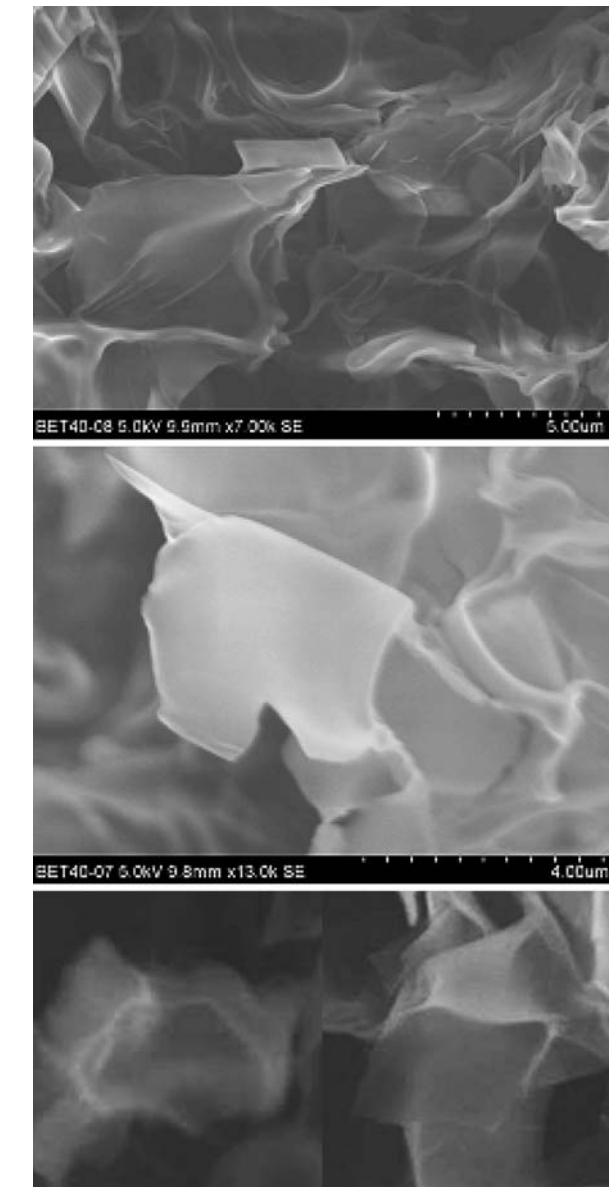

Fig. 3 SEM images of BET400. The bottom images shown in magnification are individual, translucent nanosheets of very small size and thickness

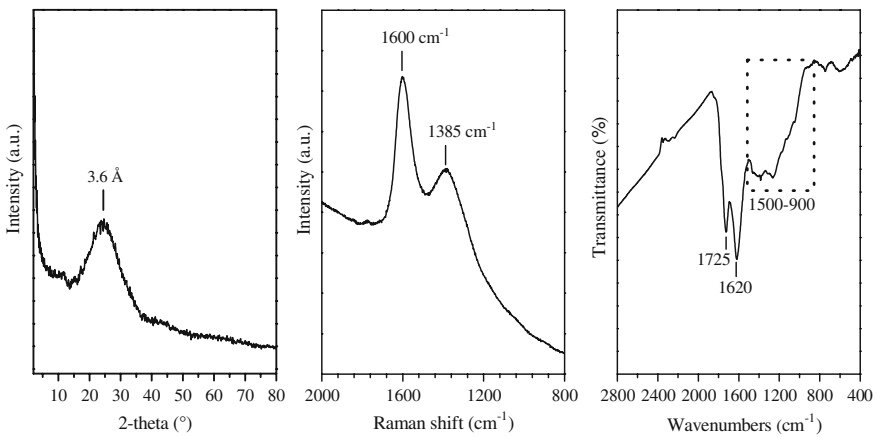

Fig. 2 XRD (*left*), Raman (*middle*), and FTIR (*right*) profiles of BET400. The band at 1620 cm^{-1} in the corresponding FTIR spectrum is due to KBr humidity

Raman spectrum of BET400 (Fig. 2, middle) shows the D band (1385 cm^{-1}) and the G band (1600 cm^{-1}), both being characteristic fingerprints of all carbon materials with a defective graphite structure [4, 5, 9]. Albeit the growth of the nanosheets was conducted in air, the G band peak is considerably stronger than the D band peak, thereby suggesting the formation of long-range graphitized carbon with a relatively small number of structural defects, the latter pertaining to vacancies, morphological sheet distortions (folding, twisting, etc.), and the presence of heteroatoms (H, O, and N). On the other hand, the FTIR spectrum of BET400 (Fig. 2, right) is consistent with that of graphite oxide showing a clear band at 1725 cm^{-1} assigned to carbonyl groups (–C=O, –COOH) along with a broad band between

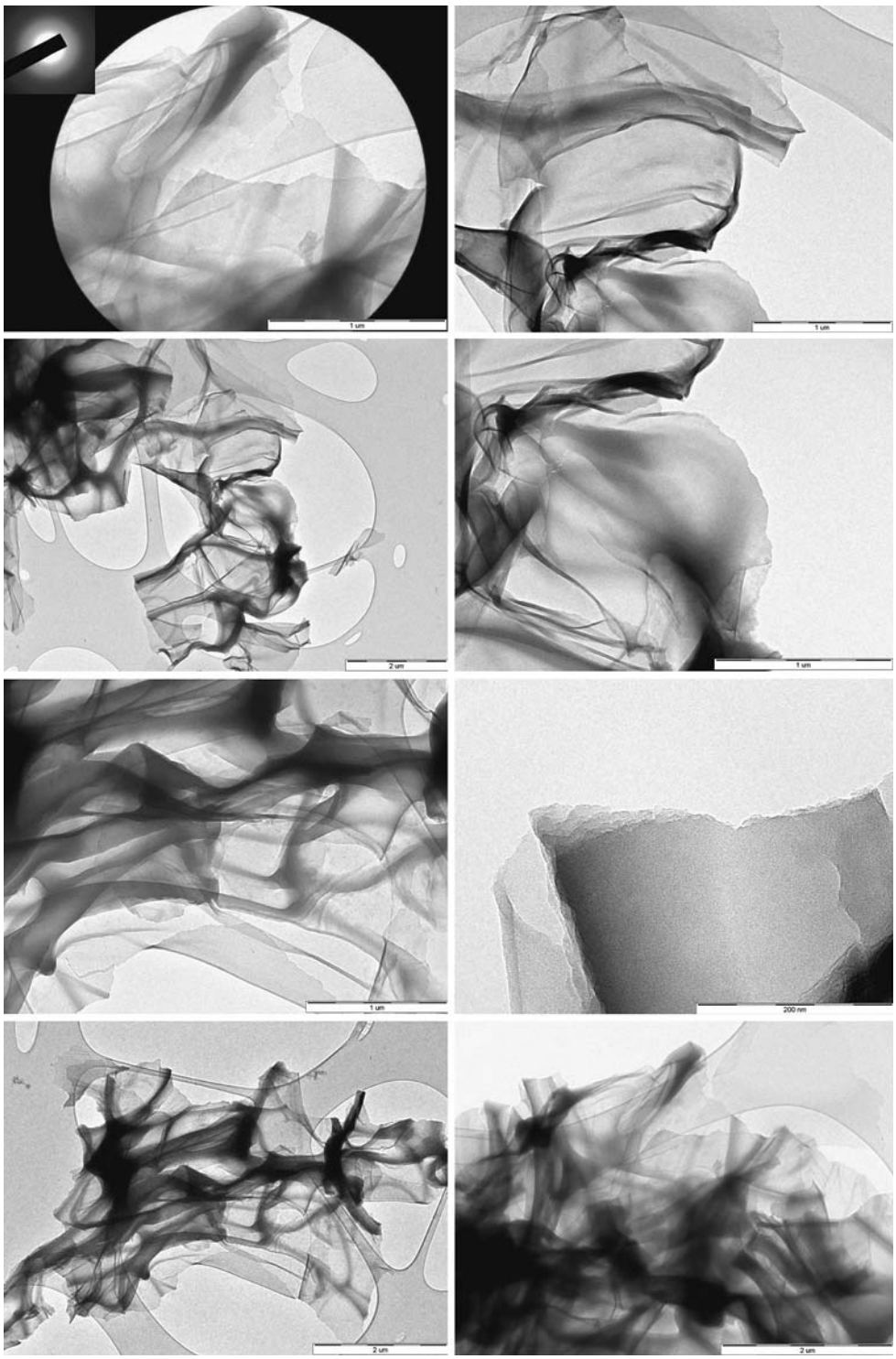

Fig. 4 TEM images of BET400 (the corresponding SAED pattern is included as inset)

1500 and 900 cm^{-1} assigned to the O–H deformations of the C–OH groups and to C–O stretching vibrations [19, 20]. Based on the XRD, FTIR, and elemental analysis results, the heteroatoms O, H, and N should be structurally incorporated within the carbon layers in the form of heterocyclic rings as well as at the periphery of the sheets in the form of surface exposed hydroxyl and carboxyl groups [20].

Microscopy studies (SEM, TEM, and AFM) reveal that BET400 is solely composed of ultrathin nanosheets less than 6 nm in thickness and 1–5 μm in lateral dimensions (>95% phase purity). More specifically, the SEM images of BET400 (Fig. 3) display assemblies of flexible thin nanosheets standing on edges with a uniform thickness along the entire plane and a smooth, occasionally translucent surface. TEM evaluation of the sample demonstrates mostly bundles of overlapped nanosheets and sporadically individual specimens, all having an isotropic amorphous structure (e.g. turbostratic disorder) according to the corresponding SAED pattern (Fig. 4). The nanosheets are a few micrometers wide but they are so thin that they seem to be transparent to electron beams. In addition, they consist of several numbers of stacked graphenes in a lamellar registry as evidenced by the multilayered structure near the edges of individual sheets (Fig. 4). The 2-D layered structure of BET400 is more pronounced in the HR-TEM analysis of the nanosheets where parallel lattice planes (or tactoids) with an interlayer distance of ~4 Å (versus 3.6 Å from XRD) can be clearly observed (Fig. 5). AFM gives a more precise estimation of the sheets thickness, with the white areas depicting highest objects of several overlapped sheets and the brown one the mica support at the bottom (Fig. 6). Thus, the uppermost point gives an impressive maximum height of 6.6 nm, demonstrating that the sheets are ultranarrow (Fig. 6). Considering that the white areas are actually assemblies of nanosheets that veiling each other, we can safely conclude that the thickness of individual sheets should be even less than 6.6 nm, presumably between 1 and 3 nm (based on XRD). In other words, the value of ~7 nm essentially reflects the thickness of nanosheet assemblies and is consistent (within the experimental error) with the thickness obtained from the surface area measurements (~9 nm). In order to better realize the AFM results, TEM is also included for comparison as a sort of "invert" image (Fig. 6). In this latter case, the dark areas (versus white in AFM) clearly correspond to overlapped sheets, whereas the light grey ones (versus brown in AFM for mica) to the carbon support at the bottom.

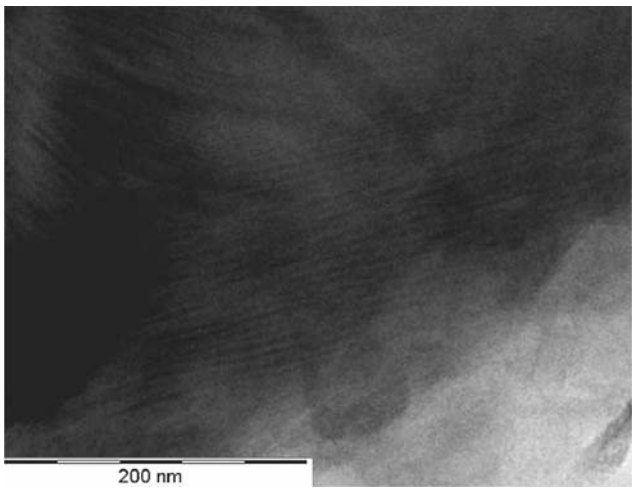

Fig. 5 HR-TEM image of BET400

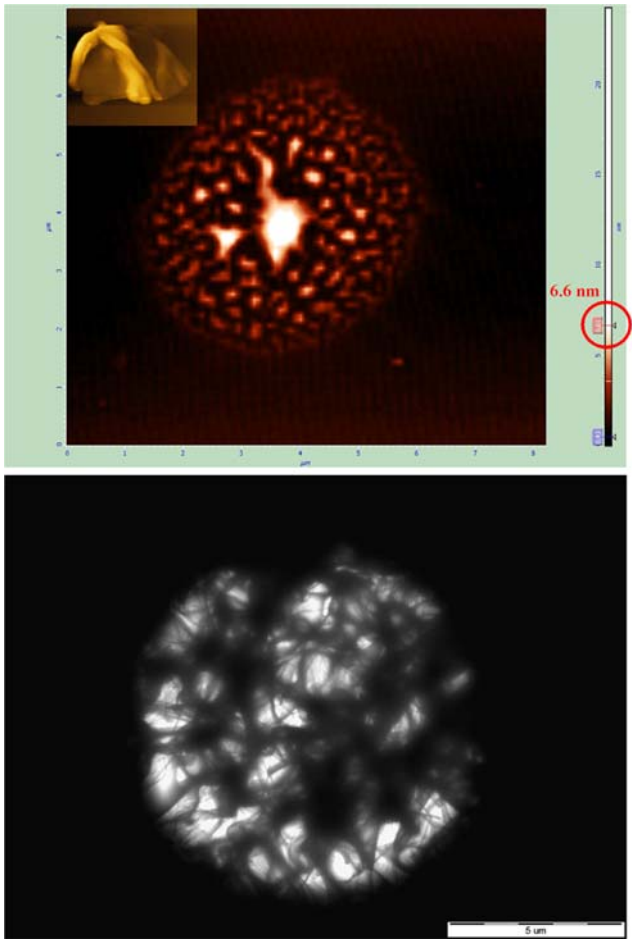

Fig. 6 AFM images of BET400 on mica substrate (inset: a standing and twisted single nanosheet). TEM is included for comparison

In summary, the efficient synthesis of ultrathin carbon nanosheets by the solid-state pyrolysis of betaine is reported. The nanosheets are less than 6 nm in thickness and 1–5 μm in lateral dimensions, highly graphitized, contain polar functional groups on the surface, and possess a relatively high specific surface area (~100 m^2 g^{-1}). The particular bottom-up approach eliminates certain drawbacks of previous methods and holds promise for the low-cost synthesis of powder carbon nanosheets.

Acknowledgements This work was supported by the projects of the ministry of education of the Czech Republic (1M6198959201 and MSM6198959218). We also thank D. Jancik and M. Vujtek for their technical assistance in the microscopy studies.

References

1. Chung DDL (2002) J Mater Sci 37:1475. doi:10.1023/A:1014915307738
2. Jang BZ, Zhamu A (2008) J Mater Sci 43:5092. doi:10.1007/s10853-008-2755-2
3. Shioyama H (2001) J Mater Sci Lett 20:499
4. Wang J, Zhu M, Outlaw RA, Zhao X, Manos DM, Holloway BC (2004) Carbon 42:2867
5. Kuang Q, Xie S-Y, Jiang Z-Y, Zhang X-H, Xie Z-X, Huang R-B, Zheng L-S (2004) Carbon 42:1737
6. Wu Y, Yang B, Zong B, Sun H, Shen Z, Feng Y (2004) J Mater Chem 14:469
7. Zhao X, Outlaw RA, Wang JJ, Zhu MY, Smith GD, Holloway BC (2006) J Chem Phys 124:194704 (6 pp)
8. Niyogi S, Bekyarova E, Itkis ME, McWilliams JL, Hamon MA, Haddon RC (2006) J Am Chem Soc 128:7720
9. Qin Y, Eggers M, Staedler T, Jiang X (2007) Nanotechnology 18:345607 (4 pp)
10. Stankovich S, Dikin DA, Piner RD, Kohlhaas KA, Kleinhammes A, Jia Y, Wu Y, Nguyen ST, Ruoff RS (2007) Carbon 45:1558
11. Peng W, Wang Z, Yoshizawa N, Hatori H, Hirotsu T (2008) Chem Commun 4348
12. Zhu J (2008) Nat Nanotechnol 3:528
13. Shang NG, Papakonstantinou P, McMullan M, Chu M, Stamboulis A, Potenza A, Dhesi SS, Marchetto H (2008) Adv Funct Mater 18:3506
14. Zhou L, Lin J, Lin H, Chen G (2008) J Mater Sci 43:4886. doi:10.1007/s10853-008-2710-2
15. Liu X, Fu D, Jia H, Xu B (2008) J Mater Sci 43:5014. doi:10.1007/s10853-008-2659-1
16. Kalaitzidou K, Fukushima H, Askeland P, Drzal LT (2008) J Mater Sci 43:2895. doi:10.1007/s10853-007-1876-3
17. Viertorinne M, Valkonen J, Pitkänen I, Mathlouthi M, Nurmi J (1999) J Mol Struct 477:23
18. Suuronen J, Pitkänen I, Halttunen H, Moilanen R (2002) J Therm Anal Calorim 69:359
19. Bourlinos AB, Gournis D, Petridis D, Szabó T, Szeri A, Dékány I (2003) Langmuir 19:6050
20. Szabó T, Berkesi O, Forgó P, Josepovits K, Sanakis Y, Petridis D, Dékány I (2006) Chem Mater 18:2740
21. Bourlinos AB, Steriotis TA, Karakassides M, Sanakis Y, Tzitzios V, Trapalis C, Kouvelos E, Stubos A (2007) Carbon 45:852
22. Stoller MD, Park S, Zhu Y, An J, Ruoff RS (2008) Nano Lett 8:3498